The Journal of Immunology

RESEARCH ARTICLE | MARCH 01 2017

MAFB Determines Human Macrophage Anti-Inflammatory Polarization: Relevance for the Pathogenic Mechanisms Operating in Multicentric Carpotarsal Osteolysis

Víctor D. Cuevas; ... et. al

J Immunol (2017) 198 (5): 2070–2081.
https://doi.org/10.4049/jimmunol.1601667

MAFB Determines Human Macrophage Anti-Inflammatory Polarization: Relevance for the Pathogenic Mechanisms Operating in Multicentric Carpotarsal Osteolysis

Víctor D. Cuevas,* Laura Anta,† Rafael Samaniego,‡ Emmanuel Orta-Zavalza,* Juan Vladimir de la Rosa,§ Geneviève Baujat,¶,‖ Ángeles Domínguez-Soto,* Paloma Sánchez-Mateos,‡ María M. Escribese,# Antonio Castrillo,§ Valérie Cormier-Daire,¶,‖ Miguel A. Vega,* and Ángel L. Corbí*

Macrophage phenotypic and functional heterogeneity derives from tissue-specific transcriptional signatures shaped by the local microenvironment. Most studies addressing the molecular basis for macrophage heterogeneity have focused on murine cells, whereas the factors controlling the functional specialization of human macrophages are less known. M-CSF drives the generation of human monocyte-derived macrophages with a potent anti-inflammatory activity upon stimulation. We now report that knockdown of MAFB impairs the acquisition of the anti-inflammatory profile of human macrophages, identify the MAFB-dependent gene signature in human macrophages and illustrate the coexpression of MAFB and MAFB-target genes in CD163$^+$ tissue-resident and tumor-associated macrophages. The contribution of MAFB to the homeostatic/anti-inflammatory macrophage profile is further supported by the skewed polarization of monocyte-derived macrophages from multicentric carpotarsal osteolysis (Online Mendelian Inheritance in Man #166300), a pathology caused by mutations in the *MAFB* gene. Our results demonstrate that MAFB critically determines the acquisition of the anti-inflammatory transcriptional and functional profiles of human macrophages. ***The Journal of Immunology*****, 2017, 198: 2070–2081.**

Macrophage heterogeneity derives from the existence of tissue-specific factors that control macrophage differentiation and functional maturation. M-CSF and IL-34 control macrophage differentiation in most tissues (1, 2), whereas GM-CSF drives the generation of alveolar macrophages (3). Circulating monocytes are recruited to damaged tissues under inflammatory conditions (4) and acquire specialized functions (macrophage polarization) under the influence of extracellular cues (5). The macrophage sensitivity to the surrounding milieu is exemplified by the ability of GM-CSF and M-CSF to induce the acquisition of distinct effector functions (6, 7). Previous studies have demonstrated that GM-CSF–primed macrophages (GM-MØ) and M-CSF–primed macrophages (M-MØ) exhibit distinct cellular phenotypes (8–11), a distinct metabolic state (12, 13), and display opposite effector functions like activin A–mediated inhibition of tumor cell growth and production of LPS-induced cytokines (7, 14). Specifically, GM-CSF primes macrophages (GM-MØ) to gain immunogenic activity and to produce inflammatory cytokines upon TLR stimulation, whereas M-CSF primes macrophages (M-MØ) with tissue repair and proangiogenic functions, and with potent TLR-induced IL-10–producing ability (7, 15). Accordingly, human GM-MØ and M-MØ are considered as proinflammatory and anti-inflammatory macrophages (6, 16).

MAFB is a transcription factor of the large MAF subfamily (MAFA, cMAF, MAFB, NRL) that binds to a specific DNA element (MARE); heterodimerizes with cMAF, JUN, and FOS (17–19); and associates and functionally inhibits MYB (19), MITF, and NFATc1 (20). MAFB controls lens development (21), lymphangiogenesis (22), pancreatic α and β cell differentiation (23, 24), skin cell differentiation (25), chondrocyte matrix formation and

*Laboratorio de Células Mieloides, Centro de Investigaciones Biológicas, Consejo Superior de Investigaciones Científicas, 28040 Madrid, Spain; †Servicio de Cirugía Ortopédica y Traumatología, Complejo Hospitalario de Santiago de Compostela, 15706 Santiago de Compostela, Spain; ‡Laboratorio de Inmuno-Oncología, Unidad de Microscopía Confocal, Instituto de Investigación Sanitaria Gregorio Marañón, 28007 Madrid, Spain; §Instituto de Investigaciones Biomedicas Alberto Sols, Consejo Superior de Investigaciones Científicas, 28029 Madrid, Spain; ¶Unidad de Biomedicina, Instituto de Investigaciones Biomédicas–Universidad de Las Palmas de Gran Canaria (ULPGC), Instituto Universitario de Investigaciones Biomedicas y Sanitarias de la ULPGC, 35001 Las Palmas, Spain; ‖Département de Génétique, INSERM U781, Université Paris Descartes-Sorbonne Paris Cité, Institut Imagine, Hôpital Necker Enfants Malades, 75015 Paris, France; and #Institute for Applied Molecular Medicine, School of Medicine, University CEU San Pablo, Madrid, Spain

ORCIDs: 0000-0002-2816-8070 (V.D.C.); 0000-0002-4196-5218 (L.A.); 0000-0002-3081-7332 (R.S.); 0000-0003-1443-7548 (J.V.d.l.R.); 0000-0003-1980-5733 (Á.L.C.).

Received for publication September 26, 2016. Accepted for publication December 16, 2016.

This work was supported by Ministerio de Economía y Competitividad (MINECO) Grant SAF2014-52423-R and Instituto de Salud Carlos III Red de Investigación en Enfermedades Reumáticas Grant RIER RD12/009 (to Á.L.C. and M.A.V.), MINECO Grant SAF2014-56819-R (to A.C.), Comunidad Autónoma de Madrid/Fonds Européen de Développement Économique et Régional RAPHYME Program Grant S2010/BMD-2350 (to Á.L.C. and A.C.), and a Formación de Personal Investigador predoctoral fellowship from MINECO through Grant BES-2012-053864 (to V.D.C.).

V.D.C., L.A., M.M.E., A.C., M.A.V., and Á.L.C. designed the research; V.D.C., L.A., R.S., E.O.-Z., J.V.d.l.R., G.B., Á.D.-S., P.S.-M., and V.C.-D. performed experiments, recruited patients, and analyzed data; V.D.C. and Á.L.C. wrote the manuscript.

The sequences presented in this article have been submitted to Gene Expression Omnibus under accession number GSE84622.

Address correspondence and reprint requests to Dr. Ángel L. Corbí and Dr. Miguel A. Vega, Centro de Investigaciones Biológicas, Consejo Superior de Investigaciones Científicas, Calle Ramiro de Maeztu 9, 28040 Madrid, Spain. E-mail addresses: acorbi@cib.csic.es (Á.L.C.) and mavega@cib.csic.es (M.A.V.)

The online version of this article contains supplemental material.

Abbreviations used in this article: GM-MØ, GM-CSF–primed macrophages; GSEA, gene set enrichment analysis; MARE, MAF recognition element; MCTO, multicentric carpotarsal osteolysis; M-MØ, M-CSF–primed macrophages; RANKL, receptor activator for NF-κB ligand; siControl, small interfering RNA control; siMAFB, MAFB-specific small interfering RNA; TRAP, tartrate-resistant acid phosphatase.

development (26), and podocyte generation (27–30), and also regulates type I IFN production through recruitment of coactivators to IFN regulatory factor 3 (31). Within the murine myeloid lineage, MafB is preferentially expressed in most tissue-resident macrophages, whose specific enhancers contain an overrepresentation of MARE sequences (32). MAFB restricts the ability of M-CSF to instruct myeloid cell proliferation, promotes macrophage differentiation (33) through repression of self-renewal enhancers in macrophages in vivo (34), and negatively regulates osteoclast generation via inhibition of FOS, MITF, and NFATc1 (20).

The deregulated expression/function of MAFB gives rise to various human pathologies. Specifically, heterozygous missense MAFB mutations result in multicentric carpotarsal osteolysis (MCTO; Online Mendelian Inheritance in Man #166300), a rare osteolytic syndrome with kidney affectation (35–38), whereas MAFB overexpression is a common feature in multiple myeloma (39) and is linked to Dupuytren's disease (40), a fibroblastic proliferation of the palmar fascia. Loss of MAFB function has recently been shown to cause Duane retraction syndrome (41). Besides, animal models of disease revealed that MafB deficiency ameliorates atherosclerotic lesions (42) and accelerates obesity (43), whereas MafB mutations cause kidney-associated diseases that result from altered podocyte differentiation (44).

Despite its pathological relevance, the association of MAFB to human macrophage polarization states and the identity of MAFB-regulated genes in human macrophages are mostly unknown. We report that MAFB determines the anti-inflammatory gene signature of M-CSF–primed human macrophages, identify the range of MAFB-dependent genes in macrophages both in vitro and in vivo, and demonstrate that MCTO monocyte-derived macrophages exhibit an exacerbated anti-inflammatory profile that might contribute to the pathological consequences of deregulated MAFB expression or function.

Materials and Methods

Generation of monocyte-derived macrophages

The methods were carried out in accordance with the approved guidelines. Human PBMC were isolated from buffy coats from normal donors over a Lymphoprep (Nycomed Pharma, Oslo, Norway) gradient according to standard procedures approved by Ethical Board of the Consejo Superior de Investigaciones Científicas. Blood leukocyte preparations were purchased from Comunidad de Madrid Blood Center. Monocytes were purified from PBMC by magnetic cell sorting using anti-CD14 microbeads (Miltenyi Biotec, Bergisch Gladbach, Germany) (>95% $CD14^+$ cells). Monocytes (0.5×10^6 cells/ml, >95% $CD14^+$ cells) were cultured in RPMI 1640 supplemented with 10% FBS for 7 d in the presence of 1000 U/ml GM-CSF, 10 ng/ml M-CSF (ImmunoTools, Friesoythe, Germany), or 10 ng/ml IL-34 (BioLegend) to generate GM-CSF–polarized macrophages (GM-MØ), M-CSF–polarized macrophages (M-MØ), or IL-34–polarized macrophages, respectively. Cytokines were added every 2 d. Cells were cultured in 21% O_2 and 5% CO_2. Monocyte-derived osteoclasts were generated by culturing monocytes for 12 d on glass coverslips in the presence of M-CSF (25 ng/ml) and receptor activator for NF-κB ligand (RANKL; 30 ng/ml). After fixing, osteoclast generation was verified by staining for tartrate-resistant acid phosphatase (TRAP) using the Leukocyte Acid Phophatase kit (Sigma-Aldrich). Determination of osteoclast-mediated degradation of human bone collagen (type I) was done using the OsteoLyse Assay kit (human collagen; Lonza, Walkersville, MD). Generation of monocyte-derived macrophages from MCTO patients was done using a similar procedure and following the Medical Ethics Committee procedures of Hospital Clínico Universitario, Santiago de Compostela (patient MCTO#1), and of Hôpital Necker Enfants Malades, Paris (two patients referred to as MCTO#2). Informed consents were obtained from all subjects. MCTO#1 patient was found to contain a $Ser^{54}Leu$ (161C > T) mutation, whereas patients MCTO#2 contain a $Pro^{63}Leu$ (188C > T) mutation (36). For MAFB knockdown, M-MØ (10^6 cell/ml) were transfected with a MAFB-specific small interfering RNA (siMAFB, 50 nM; Life Technologies) using Hiperfect (Qiagen). As a control, cells were transfected with a nonspecific small interfering RNA control (siControl; Life Technologies). After transfection, cells were cultured for the indicated times in RPMI 1640 supplemented with 10% FBS. Where indicated, cells were treated with 10 ng/ml *Escherichia coli* 055:B5 LPS (Sigma-Aldrich) or exposed to tumor ascitic fluids of different origins (11) that were provided by M. Palomero (Oncology Department, Hospital General Universitario Gregorio Marañón). Macrophage supernatants were assayed for the presence of cytokines using commercial ELISA kits for CCL2 (BD Biosciences) and IL-10 (BioLegend), according to the protocols supplied by the manufacturers. Mouse bone marrow–derived macrophages were generated using human M-CSF (10 ng/ml; ImmunoTools). All animal procedures were approved by the Comité Ético de Experimentación Animal (Ethical Committee for Animal Experimentation) of the Consejo Superior de Investigaciones Científicas and conducted in accordance with the approved guidelines.

Quantitative real-time RT-PCR

Total RNA was extracted using the NucleoSpin RNA/Protein kit (Macherey-Nagel, Düren, Germany), retrotranscribed, and amplified using the Universal Human Probe Library (Roche Diagnostics, Mannheim, Germany). Oligonucleotides for selected genes were designed according to the Roche software for quantitative real-time PCR (Roche Diagnostics, Mannheim, Germany). Assays were made in triplicate, and results were normalized according to the expression levels of *TBP* or 18S rRNA for macrophage or monocyte samples, respectively. Custom-made microfluidic gene cards (Roche Diagnostics) were designed to analyze the expression of a set of genes whose expression is differentially modulated by LPS in GM-MØ and M-MØ (V.D. Cuevas and A.L. Corbí, unpublished observations). Specifically, the gene cards included 10 genes upregulated by LPS in both GM-MØ and M-MØ, 16 genes upregulated by LPS exclusively in GM-MØ, 37 genes upregulated by LPS exclusively in M-MØ, 3 genes downregulated by LPS exclusively in GM-MØ, and 20 genes downregulated by LPS exclusively in M-MØ. Assays were made in duplicate on three independent samples of each type, and the results were normalized according to the mean of the expression level of endogenous reference genes *HPRT1*, *TBP*, and *RPLP0*. In all cases (quantitative real-time PCR or gene cards), the results were expressed using the ΔΔ cycle threshold method for quantitation.

Western blot

Cell lysates were obtained in radioimmunoprecipitation assay buffer (10 mM Tris-HCl [pH 8], 150 mM NaCl, 1% Nonidet P-40, 2 mM Pfabloc, 2 mg/ml aprotinin/antipain/leupeptin/pepstatin, 10 mM NaF, and 1 mM Na_3VO_4). A total of 10 μg cell lysate was subjected to SDS-PAGE under reducing (MAFB) or nonreducing (CLEC5A) conditions and transferred onto an Immobilon polyvinylidene difluoride membrane (Millipore). Protein detection was carried out using Abs against MAFB (sc-10022; Santa Cruz) and CLEC5A (MAB2384; R&D Systems). Protein loading was normalized using a mAb against GAPDH (sc-32233; Santa Cruz).

MAFB expression vectors, site-directed mutagenesis, and reporter assays

The coding sequence of MAFB was amplified by PCR from reverse-transcribed cDNA from a healthy donor and was sequenced to confirm the absence of mutations. The oligonucleotides used for amplification of the MAFB coding region were 5′-CGGAATTCCGATGGCCGCGGAGCTGAGC-3′ and 5′-GCTCTAGAGCTCACAGAAAGAACTCGGGAGAG-3′, which include EcoRI and XbaI restriction sites for subsequent cloning into EcoRI- and XbaI-cut pCDNA3.1(+) expression vector (pMAFBwt). Site-directed mutagenesis was carried out using the QuikChange site-directed mutagenesis kit (Stratagene) to generate MAFB expression constructs with the $Ser^{54}Leu$ mutation (161C > T, found in MCTO#1 patient) (pMAFB161T), the $Pro^{63}Arg$ mutation (188C > G) (pMAFB188G) (36), or the $Pro^{71}Ser$ mutation (211C > T) (pMAFB211T) (38). The oligonucleotides used for mutagenesis were S54L forward (5′-CACGCCTGCAGCCAGCCGGCTTGGTGTCCTCCAC-3′), S54L reverse (5′-GTGGAGGACACCAAGCCGGCTGGCTGCAGGCGTG-3′), P63R forward (5′-CCGCTCAGCACTCGGTGTAGCTCCGTGCCCTCGTC-3′), P63R reverse (5′-GACGAGGGCACGGAGCTACACCGAGTGCTGAGCGG-3′), P71S forward (5′-GTAGCTCCGTGCCCTCGTCGTCCAGCTTCAGCCCGACCGAAC-3′), and P71S reverse (5′-GTTCGGTCGGGCTGAAGCTGGACGACGAGGGCACGGAGCTAC-3′). The resulting plasmids were verified by sequencing.

To check the transcriptional activity of MAFB MCTO-causing mutations, HEK293T cells were seeded in 24-well plates at 4×10^4 cells per well and transfected with SuperFect (Qiagen) with 200 ng each expression vector and 1 μg 3×MARE-Luc reporter vector. Each transfection also included 25 ng construct expressing the *Renilla* luciferase for normalization of transfection efficiency. After 24 h, firefly and *Renilla* luciferase activities were determined by using the Dual-Luciferase Reporter Assay System (Promega). The 3×MARE-Luc reporter construct was generated by inserting three multimerized MAF-recognition elements (MARE) (18) into HindIII- and XhoI-cut pXP2-TATA plasmid. The sequences of the oligonucleotides used to generate the 3×MARE-Luc construct were

5′-agctttcgacccgaaaggTGCTGAcgTCAGCAgctagccctcgacccgaaaggTGCTGAcgTCAGCAgctagccctcgacccgaaaggTGCTGAcgTCAGCAgctagcccc-3′ and 5′-tcgaggggcta gcTGCTGAcgTCAGCAcctttcgggtcgagggctagcTGCTGAcgTCAGCAcctttcgggtcgagggctagcTGCTGAcgTCAGCAcctttcgggtcgaa-3′, in which capital letters indicate the MAFB binding sites.

To assess the protein stability of MAFB MCTO-causing mutants, HEK293T cells were transfected with 1 μg pMAFBwt, pMAFB161T, pMAFB188G, or pMAFB211T plasmids using SuperFect (Qiagen). After 24 h, cells were treated with 10 μg/ml cycloheximide, and cell lysates were generated at the indicated times using radioimmunoprecipitation assay buffer.

Microarray analysis

Global gene expression analysis was performed on RNA obtained from siControl-transfected M-MØ, siMAFB-transfected M-MØ, and M-MØ generated from either MCTO#1 or two healthy individuals. In the case of M-MØ from MCTO#1, two RNA aliquots were analyzed in parallel. RNA was isolated using the RNeasy Mini kit (Qiagen, Germantown, MD) and analyzed with a whole human genome microarray from Agilent Technologies (Palo Alto, CA). Only probes with signal values >60% quantile in at least one condition were considered for the differential expression and statistical analysis. Statistical analysis for differential gene expression was carried out using empirical Bayes moderated *t* test implemented in the limma package (http://www.bioconductor.org). For the gene expression analysis of the siMAFB-transfected M-MØ, a paired *t* test was used. The *p* values were further adjusted for multiple hypotheses tested using the Benjamini-Hochberg method to control the false discovery rate (45). All of the above procedures were coded in R (http://www.r-project.org). Microarray data were deposited in the Gene Expression Omnibus (http://www.ncbi.nlm.nih.gov/geo/) under accession number GSE84622. The differentially expressed genes in both microarray experiments were analyzed for annotated gene set enrichment using the online tool ENRICHR (http://amp.pharm.mssm.edu/Enrichr/) (46, 47). Enrichment terms were considered significant when they had a Benjamini-Hochberg–adjusted *p* value <0.05. For gene set enrichment analysis (GSEA) (48), the gene sets contained in the Molecular Signature databases available at the GSEA Web site and the previously defined proinflammatory gene set and anti-inflammatory gene set (49), which contain the top and bottom 150 probes from the GM-MØ versus M-MØ limma analysis of the microarray data in GSE68061 (ranked on the basis of the value of the *t* statistic), were used.

Fluorescence confocal microscopy

Human biopsied samples were obtained from patients undergoing surgical treatment and following the Medical Ethics Committee procedures of Hospital General Universitario Gregorio Marañón, Madrid, and Hospital Clinic, Barcelona. Frozen samples were cryosectioned (5 μm), fixed with acetone, blocked with human Igs, and simultaneously stained with different primary Abs at 1–5 μg/ml. Imaging was performed with the glycerol ACS APO ×20 NA 0.60 immersion objective of a confocal fluorescence microscope (SPE; Leica Mycrosystems). For quantification of in vivo protein expression, mean fluorescence intensities of the proteins of interest (MAFB, CD163L1, HTR2B, and CXCL12) were quantified at segmented $CD163^+$ macrophages using the FIJI software (National Institutes of Health) and background subtracted data from at least three different fields displayed as scatter plots (GraphPad). The Abs used were the following: goat polyclonal anti-MAFB (sc-10022; Santa Cruz), mouse monoclonal anti-CD163 (K0147-4; MBL), rabbit polyclonal anti-CD163L1 (HPA015663; Sigma-Aldrich), rabbit polyclonal anti-CXCL12 (P87B; PeproTech), and rabbit polyclonal anti-HTR2B (sc-25647; Santa Cruz).

Statistical analysis

For comparison of means, and unless otherwise indicated, statistical significance of the generated data was evaluated using the Student *t* test. In all cases, a *p* value < 0.05 was considered statistically significant.

Results

MAFB expression in human macrophages under homeostatic and anti-inflammatory conditions

Transcriptional analysis of M-MØ and GM-MØ (GSE27792) (14) revealed the preferential expression of the *MAFB* gene in macrophages with anti-inflammatory potential, as M-MØ express 19 times higher levels of *MAFB* RNA than GM-MØ ($p < 0.0005$) (Fig. 1A). In agreement with the transcriptional data, M-MØ exhibited much higher levels of MAFB protein than GM-MØ (Fig. 1B). During M-CSF–driven differentiation, *MAFB* mRNA levels dropped at early time points and peaked 24–48 h after M-CSF treatment (Fig. 1C, upper panel). The MAFB protein levels were greatly increased along M-MØ differentiation, with maximal levels observed 24–48 h after the initial M-CSF treatment (Fig. 1C, lower panel). Interestingly, maximal MAFB protein levels preceded the maximal level of expression of paradigmatic M-MØ–specific genes like *HTR2B*, *F13A1*, *OLFML2B*, *IL10*, and *CD163L1*, which were expressed at high levels 72 h after addition of M-CSF (Supplemental Fig. 1A). Therefore, the presence of high levels of MAFB precedes the maximal expression of M-MØ–specific genes. High levels of *MAFB* mRNA were also detected in IL-34–polarized macrophages (Fig. 1D), and MAFB levels were upregulated in monocytes exposed to M-CSF–containing tumor cell-conditioned media (Fig. 1E). Therefore, M-CSF–, IL-34–, and M-CSF–containing ascitic fluids increase MAFB expression in human monocytes. Immunohistochemistry analysis revealed that MAFB expression is absent in $CD163^+$ placenta macrophages, but readily detected in vivo in tissue-resident $CD163^+$ macrophages from colon (submucosa and muscle) and skin, as well as in tumor-associated $CD163^+$ macrophages in melanoma samples (Fig. 1F), thus confirming the expression of MAFB in certain tissue-resident macrophages and in macrophages with anti-inflammatory potential under pathological conditions. These results indicate that MAFB expression characterizes human macrophages with homeostatic/anti-inflammatory functions both in vitro and in vivo.

MAFB controls the acquisition of the anti-inflammatory transcriptional profile of M-MØ

To assess the role of MAFB in human macrophage anti-inflammatory polarization, MAFB expression was silenced using MAFB-specific small interfering RNA (siMAFB, Fig. 2A), and the effects of MAFB silencing on the M-MØ–specific transcriptome were determined. MAFB knockdown resulted in diminished expression of most M-MØ–specific genes (Fig. 2B), including *HTR2B*, *IGF1*, *STAB1*, and *CD163L1*, whose expression is associated with macrophage anti-inflammatory functions (9, 10, 49–51). A similar result was observed after Mafb knockdown in M-CSF–dependent bone marrow–derived mouse macrophages (Supplemental Fig. 1B, 1C). Therefore, MAFB controls the expression of genes associated with anti-inflammatory macrophage polarization. To identify the whole range of MAFB-dependent genes in human macrophages, we next determined the transcriptome of MAFB-deficient M-MØ (Fig. 3A). Defective MAFB expression significantly (adjusted *p* value <0.05) altered the expression of 284 probes (247 annotated genes) in M-MØ (Supplemental Table I). Specifically, MAFB knockdown led to downregulation of 147 genes and upregulation of 100 genes in M-MØ (Fig. 3B, Supplemental Table I). These results were later confirmed by quantitative PCR, which showed that MAFB silencing reduces the expression of M-MØ–specific genes (e.g., *IL10*, *CCL2*, *EMR1*, *SLC40A1*) and also increases the expression of genes associated with GM-CSF–driven proinflammatory polarization (e.g., *CLEC5A*) (50) (Fig. 3C, 3D). Gene Ontology analysis of the genes downregulated upon MAFB knockdown revealed a significant enrichment of genes upregulated by IL-10 (adjusted $p = 7.4 \times 10^{-23}$) and IFN-β (adjusted $p = 9.8 \times 10^{-32}$), but downregulated upon MYB overexpression (adjusted $p = 5.8 \times 10^{-14}$), thus supporting the link between MAFB and the expression of anti-inflammatory genes, and in line with previously reported MAFB functions and interactions (Supplemental Fig. 2A, 2B). Regarding the genes whose expression increases after MAFB knockdown, ENRICHR revealed enrichment of genes with functional MYB binding sites (adjusted $p = 5.1 \times 10^{-16}$) as well as vitamin D3– or retinoic acid–responsive genes (adjusted $p = 3.4 \times 10^{-3}$ and 5.4×10^{-3}, respectively) (Supplemental Fig. 2A, 2B), two compounds that control osteoclast

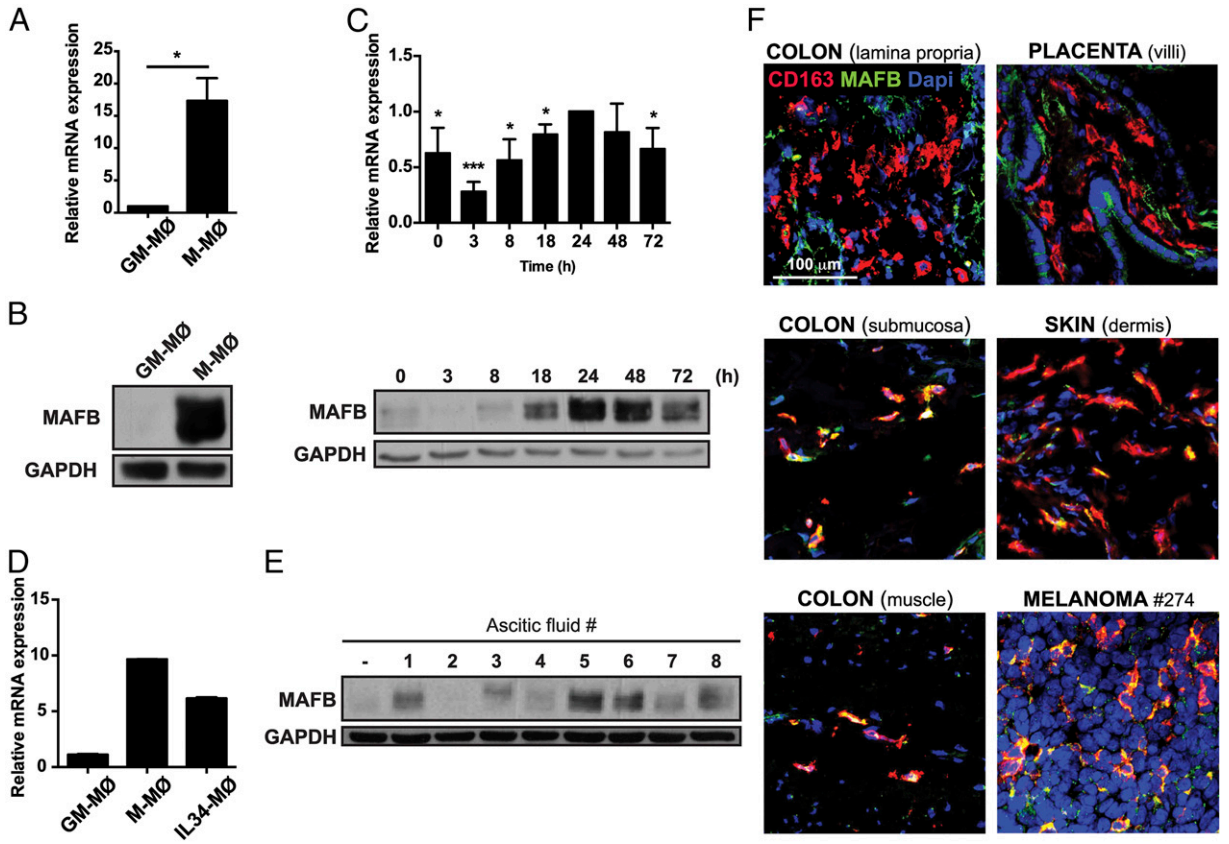

FIGURE 1. MAFB expression in homeostatic and anti-inflammatory macrophages in vitro and in vivo. (**A**) *MAFB* mRNA expression as determined by quantitative RT-PCR. Results are indicated as the expression in M-MØ relative to GM-MØ ($n = 6$, $p = 0.0055$). (**B**) MAFB protein expression as determined by Western blot. A representative experiment of three independent experiments is shown. (**C**) *MAFB* mRNA (upper panel) and protein (lower panel) expression in monocytes differentiated in the presence of M-CSF. The upper panel shows mean ± SD of the mRNA levels at the indicated time points and relative to the levels detected at the 24-h time point ($n = 4$, $*p < 0.05$, $***p < 0.005$). The lower panel illustrates the result of one of two independent experiments. (**D**) *MAFB* mRNA expression in IL-34 MØ. Shown is a representative experiment run in triplicates by quantitative RT-PCR. Results are indicated as the levels of *MAFB* mRNA relative to the levels of housekeeping *HPRT1*, *TBP*, and *RPLP0* genes. (**E**) MAFB protein in untreated monocytes (lane -) and monocytes exposed for 48 h to ascitic fluids from patients with tumors of distinct origin: bladder (lane 1), colon (lanes 2, 3, and 6), stomach (lane 4), ovary (lane 5), bile duct (lane 7), and thyroid gland (lane 8). (**F**) MAFB (green) expression in $CD163^+$ (red) macrophages in tissues. DAPI staining is shown in blue. Melanoma #274 refers to a biopsy from a lymph node melanoma metastasis sample.

proliferation and differentiation (52). Moreover, MAFB knockdown downregulated the expression of 69 genes whose mouse orthologous have been identified as MAFB targets by ChIP-sequencing (34) (Supplemental Fig. 2C, 2D).

GSEA using the gene sets that best define the proinflammatory GM-MØ– and anti-inflammatory M-MØ–specific signatures (49) revealed that MAFB knockdown significantly downregulates the expression of the genes within the M-MØ–specific gene set while increasing the expression of the GM-MØ–specific gene set (Fig. 3E). In fact, 19.4% of the genes within the M-MØ–specific gene set (33 of 170) were downregulated upon MAFB knockdown, whereas no gene within the GM-MØ–specific gene set was downregulated after MAFB silencing (Fig. 3F). These results were validated at the protein level, as MAFB knockdown reduced the basal production of both CCL2 (Fig. 3G) and IL-10 (Fig. 3H) from M-MØ. Altogether, the above results demonstrate that MAFB is a critical factor for the acquisition/maintenance of the anti-inflammatory transcriptome of human macrophages, as it positively controls the expression of M-MØ–specific genes and impairs the expression of genes associated with the GM-CSF–directed proinflammatory polarization. Such a conclusion is further supported by the significant enrichment of the hallmark-inflammatory response, hallmark IFN-γ response, and hallmark IFN-α response GSEA gene sets within the genes upregulated after siMAFB transfection (false discovery rate q value = 0).

The M-MØ–specific macrophage transcriptome is altered in macrophages derived from MCTO monocytes

Mutations within the MAFB transcriptional activation domain cause MCTO (Online Mendelian Inheritance in Man #166300), a very rare autosomal dominant disorder (35–38). Because MCTO-causing MAFB mutations map to the GSK3 phosphorylation sites (35–38) that determine large MAF protein stability (53, 54), we undertook the characterization of MCTO monocyte-derived macrophages as a means to address the consequences of an enhanced expression of MAFB within a pathological context. Specifically, we derived macrophages from a case of MCTO previously characterized from the clinical point of view (harboring a heterozygous 161C > T mutation [$Ser^{54}Leu$], and hereafter termed MCTO#1) (Fig. 4A) (55) and two previously described patients (harboring a heterozygous 188C > T mutation [$Pro^{63}Leu$], both referred to as MCTO#2) (36, 38) (Fig. 4B). MAFB protein levels were higher in both MCTO#1 monocytes (Fig. 4C) and MCTO#1 monocyte-derived macrophages (Fig. 4D), suggesting that MCTO MAFB mutations enhance protein stability. In line with this hypothesis, MAFB mutants containing the mutations found in MCTO#1 and two additional patients (188C > G, [Pro^{63} Arg] and 211C > T, [$Pro^{71}Ser$], respectively) (36, 38) exhibited a considerably extended $t_{1/2}$ after transfection in HEK293T cells (Fig. 4E). Besides, and in agreement with previous results on

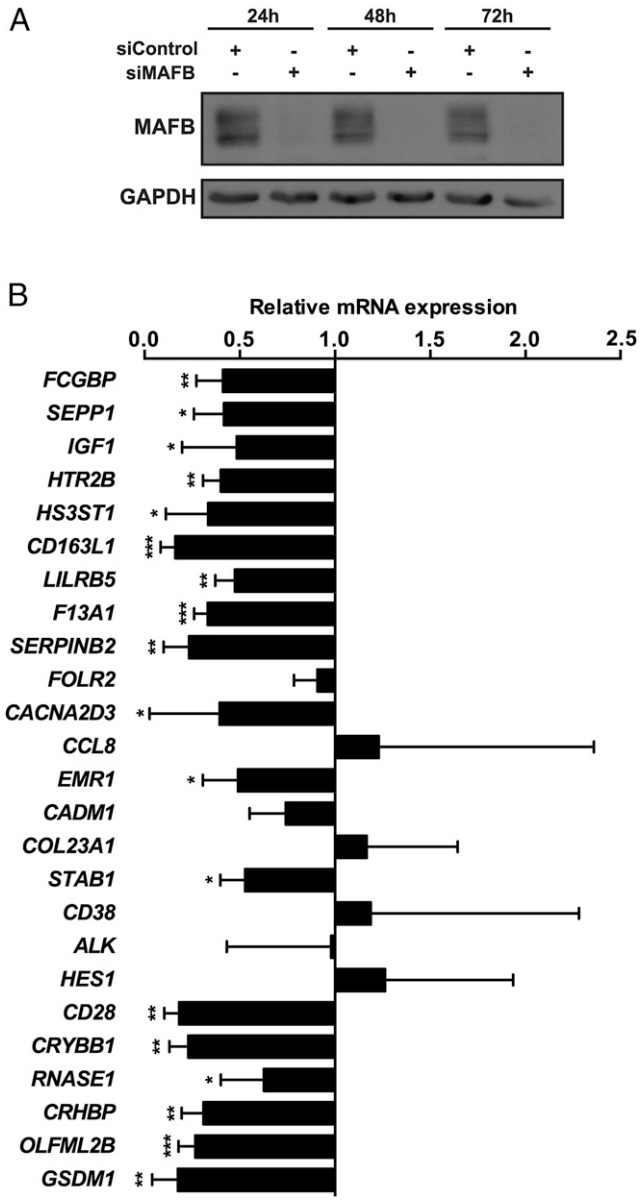

FIGURE 2. The expression of M-MØ–specific genes is MAFB dependent. (**A**) MAFB Western blot in siControl or siMAFB M-MØ for the indicated times. (**B**) Quantitative RT-PCR of the indicated genes after transfection for 24 h. Results are indicated as the mRNA levels of each gene in siMAFB M-MØ relative to siControl cells ($n = 4$, $*p < 0.05$, $**p < 0.005$, $***p < 0.0005$).

MAF and MAFA (17, 54), MCTO MAFB mutants exhibited reduced transactivation activity (Fig. 4F). Therefore, MCTO monocytes constitute a useful, and pathologically relevant, system to test the transcriptional consequences of an enhanced MAFB expression in human macrophages. Accordingly, M-MØ and GM-MØ were generated from MCTO#1 monocytes, and the transcriptomic profile of MCTO#1 M-MØ was determined. Comparison of MCTO#1 and control M-MØ gene signatures revealed the differential expression (adjusted $p < 0.19$, corresponding to unadjusted $p < 0.005$) of 321 annotated genes, with 231 genes downregulated and 90 genes upregulated in MCTO#1 M-MØ (Fig. 5A, Supplemental Table II). Analysis of the genes with lower expression in MCTO#1 M-MØ revealed a significant enrichment of genes containing functional MYB (adjusted $p = 4.5 \times 10^{-9}$), MITF (adjusted $p = 7.5 \times 10^{-13}$), and JUN binding sites (adjusted $p = 6.5 \times 10^{-8}$) (Fig. 5B), what fits with the known inhibitory actions of MAFB (20). Further supporting the presence of elevated MAFB levels in MCTO M-MØ, the set of genes with lower expression in MCTO#1 M-MØ was enriched in genes positively regulated by RANKL (adjusted $p = 1.9 \times 10^{-13}$), a major driver of osteoclast generation (20) (Fig. 5B). Interestingly, the set of genes with higher expression in MCTO M-MØ was enriched in genes downregulated in systemic juvenile idiopathic arthritis (adjusted $p = 2.5 \times 10^{-2}$), a pathology that mimics MCTO (56). Further validation of microarray data through quantitative RT-PCR on independent samples of MCTO#1 and MCTO#2 M-MØ allowed the identification of 14 genes whose expression is significantly different between control and MCTO-derived M-MØ (Fig. 5C).

The global transcriptional effect of MCTO-causing MAFB mutations was also assessed by GSEA using the gene sets that best define GM-MØ– and M-MØ–specific signatures. MCTO#1 M-MØ exhibited a significant reduction in the expression of proinflammatory (GM-MØ–specific) genes as well as a significant increase in the expression of anti-inflammatory (M-MØ–specific) genes (Fig. 5D), with genes such as *IL-10*, *HTR2B*, and *CD209* critically contributing to these significant changes. In fact, the expression of these and other M-MØ–specific genes was also significantly enhanced in M-MØ from MCTO#1 and MCTO#2 monocytes (Fig. 5E). Conversely, and in line with the GSEA results, the expression of genes that best define proinflammatory GM-MØ polarization (*TNF*, *CCR2*, *INHBA*, *EGLN3*) (9, 12, 14) appeared reduced, whereas *IL10* was enhanced, in MCTO#1 GM-MØ (Fig. 5F). Moreover, in agreement with the inhibitory effect of the MCTO#1 MAFB mutation on the expression of RANKL-regulated genes (Fig. 5B), MCTO#1 monocytes exposed to M-CSF and RANKL exhibited an impaired ability to differentiate into multinucleated osteoclasts, as shown by TRAP5 staining (Fig. 5H), expression of osteoclast differentiation gene markers (*CTSK*, *OCSTAMP*, *DCSTAMP*, and the TRAP-encoding gene *ACP5*) (Fig. 5I), and collagen-degradation ability (Fig. 5J). Altogether, these results indicate that macrophages from MCTO patients exhibit an enhanced anti-inflammatory profile and that heterozygous MCTO-causing MAFB mutations drive macrophages toward the upregulation of genes associated with anti-inflammatory macrophage polarization, thus reinforcing the contribution of MAFB to the acquisition and maintenance of the anti-inflammatory gene signature in human macrophages (Fig. 5G).

MAFB also influences the LPS responsiveness of human macrophages

Next, the involvement of MAFB in the LPS-induced activation of M-MØ was assessed through the analysis of the M-MØ–specific transcriptional response to LPS, which differs from that of GM-MØ and includes *CCL19*, *ARNT2*, *MAOA*, and *PDGFA* upregulation (V.D. Cuevas and A.L. Corbí, unpublished observations). MAFB knockdown altered the LPS responsiveness of M-MØ, as it reduced the LPS-dependent upregulation of *CCL19*, *ARNT2*, *PDGFA*, and *MAOA* (Fig. 6A) and significantly diminished the LPS-induced expression of *IL10* (Fig. 6B). By contrast, the LPS-mediated increase of these genes was higher in MCTO#1 M-MØ than in control M-MØ (Fig. 6C), again illustrating the opposite consequences of MAFB silencing and MCTO-causing MAFB mutations. Therefore, MAFB also contributes to the acquisition of the gene expression profile of LPS-activated M-MØ.

Coexpression of MAFB and MAFB-regulated genes in human macrophages in vivo

To gain additional evidence for the physiological significance of the MAFB-dependent transcriptome in human macrophages, we next

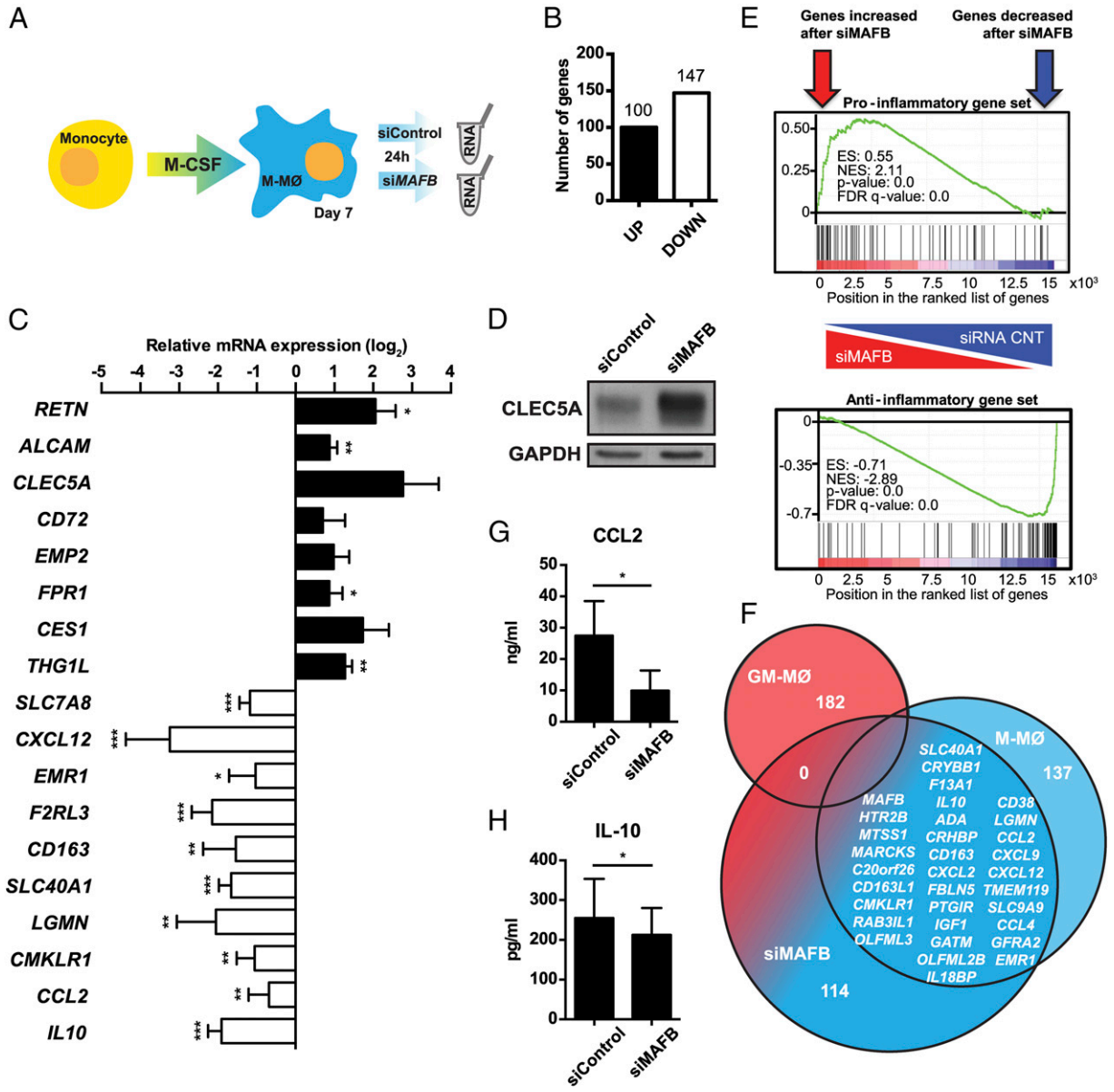

FIGURE 3. MAFB controls the global anti-inflammatory transcriptional signature of M-MØ. (**A**) Experimental design. (**B**) Number of genes whose expression is higher (UP) or lower (DOWN) in siMAFB M-MØ compared with siControl M-MØ (adjusted $p < 0.05$). (**C**) Validation of microarray results by quantitative RT-PCR in independent samples of siMAFB and siControl M-MØ ($n = 4$, $*p < 0.05$, $**p < 0.005$, $***p < 0.0005$). Data are indicated as mean ± SD of mRNA levels in siMAFB M-MØ relative to siControl M-MØ. (**D**) CLEC5A Western analysis in M-MØ treated as indicated. Shown is one experiment of three performed on independent samples. (**E**) GSEA analysis on the *t* statistic–ranked list of genes obtained from the siMAFB–M-MØ versus siControl–M-MØ limma analysis, using the proinflammatory (top) and anti-inflammatory (bottom) gene sets previously defined (49). Red and blue arrows indicate the location in the ranked list of those genes whose expression is higher or lower, respectively, in siMAFB M-MØ. (**F**) Venn diagram analysis of the genes with significantly lower expression in siMAFB M-MØ compared with the GM-MØ– and M-MØ–specific gene signatures (genes that are differentially expressed between GM-MØ and M-MØ by >8-fold, GSE68061). (**G** and **H**) ELISA of CCL2 and IL-10 protein levels in culture media from M-MØ treated as indicated ($n = 4$ for CCL2, $n = 7$ for IL-10, $*p < 0.05$).

determined whether a correlation exists between the expression of MAFB and proteins encoded by MAFB-dependent genes in human macrophages in vivo. To that end, we performed immunofluorescence on melanoma, in which accumulation of tumor-promoting and immunosuppressive macrophages associates with a poor clinical outcome (57), as well as in other tissues in which macrophages display anti-inflammatory/homeostatic functions (58). Coexpression of MAFB and CD163L1 was observed in $CD163^+$ macrophages from colon and dermis, where MAFB expression had been detected (Fig. 7A). Moreover, $CD163^+$ tumor-associated macrophages from melanoma samples coexpressed MAFB and the proteins encoded by MAFB-dependent genes such as *HTR2B*, *CD163L1*, and *CXCL12* (Fig. 7B). Therefore, MAFB is a primary driver of the anti-inflammatory gene profile of human M-CSF–dependent macrophages, and the presence of MAFB-regulated genes provides useful markers for the in vivo identification of anti-inflammatory macrophages.

Discussion

Whereas most studies on the functional heterogeneity of macrophages have focused on mouse tissue-resident macrophages (32, 59, 60), determining the factors that underlie human macrophage heterogeneity under homeostatic and pathological conditions is still required for translational approaches to be undertaken (61).

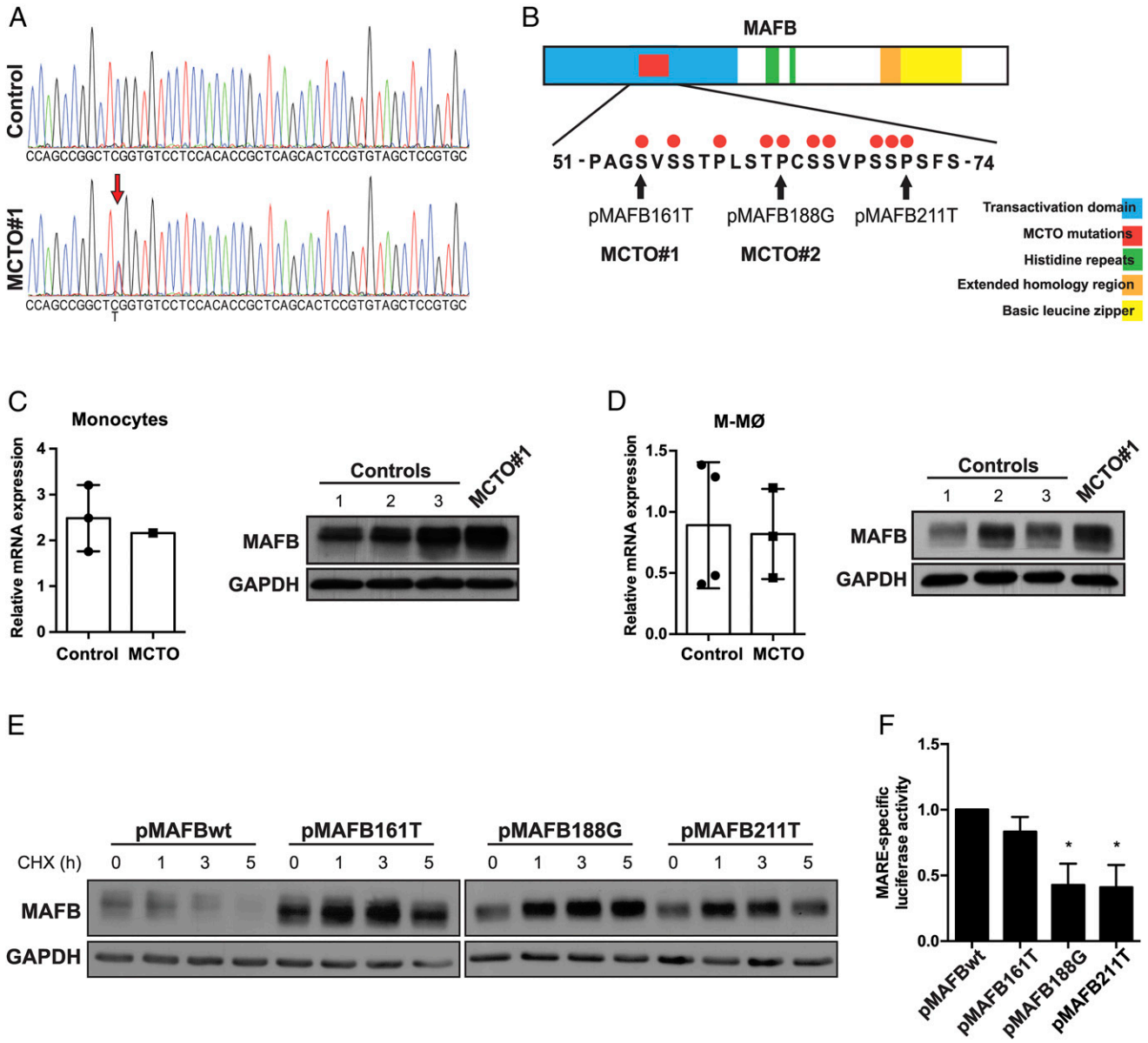

FIGURE 4. Mutations responsible for MCTO affect the stability and transcriptional activity of MAFB. (**A**) Nucleotide sequence of the mutation hotspot in the *MAFB* gene in MCTO. Sequencing of a healthy donor (top) and the MCTO#1 patient (down) is shown. Red arrow marks the heterozygous mutation (161C > T) in MCTO#1. (**B**) Representation of the MAFB protein. Red dots indicate amino acids mutated in MCTO. Black arrows indicate the amino acids mutated in the MCTO MAFB expression vectors and the amino acids affected in the MCTO#1 and MCTO#2 patients. (**C** and **D**) MAFB mRNA and protein expression in monocytes (C) and M-MØ (D) from MCTO#1 and three healthy controls, as determined by quantitative RT-PCR and Western blot. Relative mRNA expression indicates the *MAFB* mRNA levels relative to the *TBP* mRNA levels in each macrophage sample. (**E**) MAFB protein levels were determined by Western blot in HEK293T transfected with the indicated expression vectors after 1–5 h of cycloheximide (CHX) treatment. (**F**) MAFB-dependent MARE-specific transcriptional activity in HEK293T cells transfected with the indicated MAFB expression vectors. The MARE-specific luciferase activity was determined by expressing the luciferase activity produced by each MAFB construct on the 3×MARE-Luc reporter relative to the luciferase activity produced by the same expression vector in the presence of the promoter-less TATA-pXP2 plasmid. In all cases, the MARE sp. act. of each MCTO-causing MAFB mutant is referred to the activity produced by pMAFBwt (arbitrarily set to 1) ($n = 3$, $^*p < 0.05$; for pMAFB161T, $p = 0.12$).

We now report the identification of the MAFB-dependent transcriptome in IL-10–producing anti-inflammatory macrophages. The analysis of the MAFB-dependent gene set in control and MCTO macrophages has led us to demonstrate that MAFB controls the acquisition of the transcriptional signature and effector functions that characterize anti-inflammatory human macrophages in vivo and in vitro. In line with the preferential expression of MAFB in IL-10–producing macrophages, the MAFB transcriptome of human M-MØ includes genes with anti-inflammatory activity and genes whose expression associates with the acquisition of macrophage anti-inflammatory activity. Among the first group, it is worth mentioning IL-10, the paradigmatic anti-inflammatory cytokine (62); CCL2, which impairs the production of inflammatory cytokines (9, 63, 64) and is controlled by MAFB in mouse myeloid cells (65); and HTR2B, whose ligation promotes an anti-inflammatory macrophage differentiation (10). The MAFB dependency of CD163L1 expression is relevant because CD163L1 marks anti-inflammatory IL-10–producing tissue-resident macrophages in healthy secondary lymphoid organs, liver, and gut, and also characterizes melanoma-associated macrophages (50). MAFB also positively regulates the expression of the *EMR1* gene, whose mouse ortologue (the F4/80 receptor-encoding *Emr1*

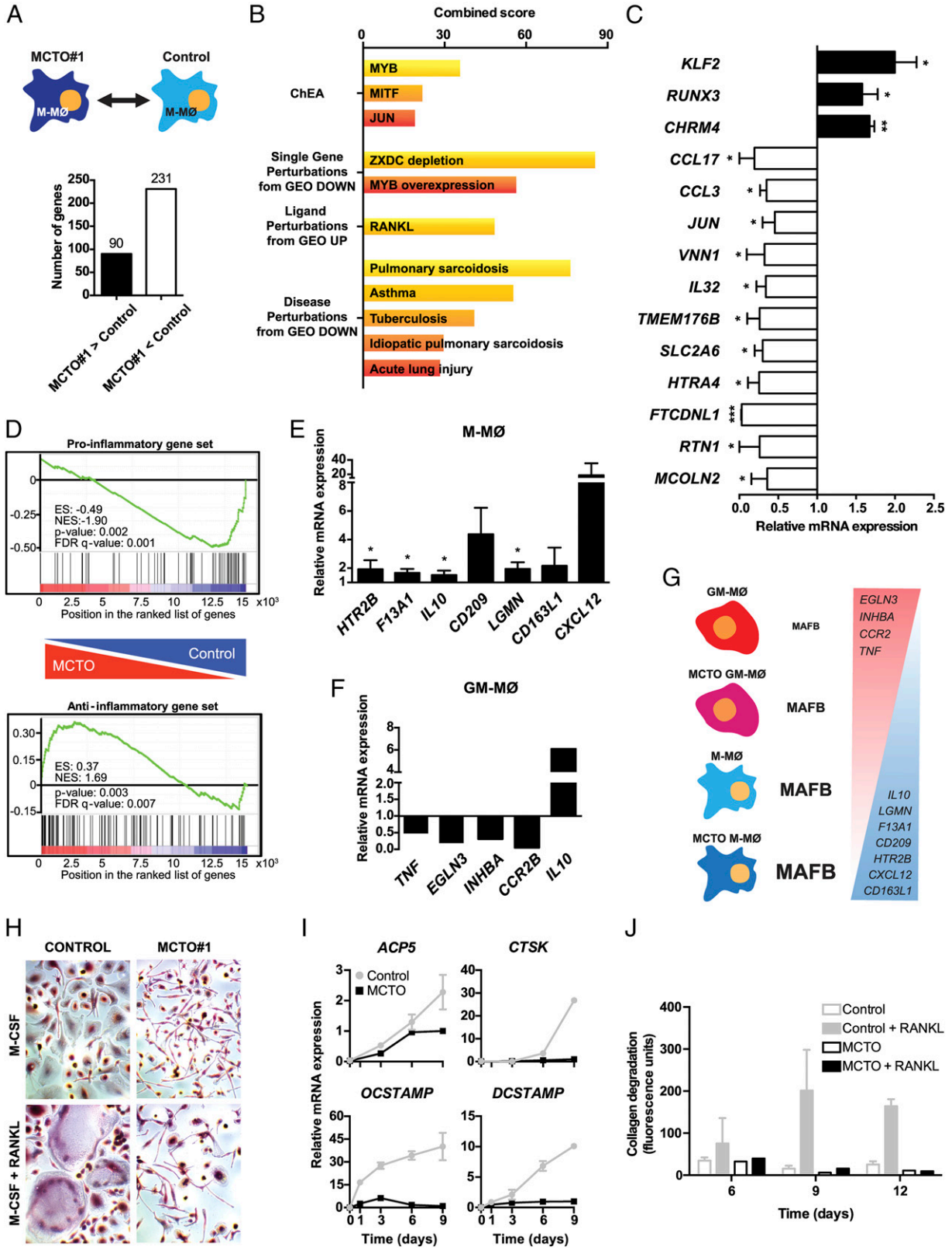

FIGURE 5. MCTO MAFB mutations significantly affect the M-MØ transcriptome. (**A**) Number of genes whose expression is higher (MCTO1 > control) or lower (MCTO1 < control) in MCTO#1 M-MØ than in control M-MØ ($p < 0.005$; adjusted $p < 0.192$; $\log_2$ fold MCTO#1/control > 0.7), as determined by microarray analysis. (**B**) Gene ontology analysis of genes downregulated in MCTO#1, using the ENRICHR tool. The results extracted from the indicated databases are shown (combined score = log(p value) × z-score). (**C**) Validation of microarray results by quantitative RT-PCR in M-MØ from MCTO#1 and MCTO#2 patients. Results are indicated as mean ± SD of mRNA levels in MCTO M-MØ relative to control M-MØ ($n = 3$, $^*p < 0.05$, $^{**}p < 0.005$, $^{***}p < 0.0005$). (**D**) GSEA analysis of the t statistic–ranked list of genes obtained from the MCTO#1 M-MØ versus control M-MØ limma analysis, using the proinflammatory (top) and anti-inflammatory (bottom) gene sets previously defined. (**E**) Expression of the indicated M-MØ–specific genes in M-MØ derived from MCTO#1 and MCTO#2 monocytes relative to control M-MØ, as determined by quantitative RT-PCR. Shown are the mean ± SD of three independent experiments ($n = 3$, $^*p < 0.05$). (**F**) Expression of the indicated GM-MØ–specific genes in MCTO#1 GM-MØ relative to control GM-MØ, as determined by quantitative (*Figure legend continues*)

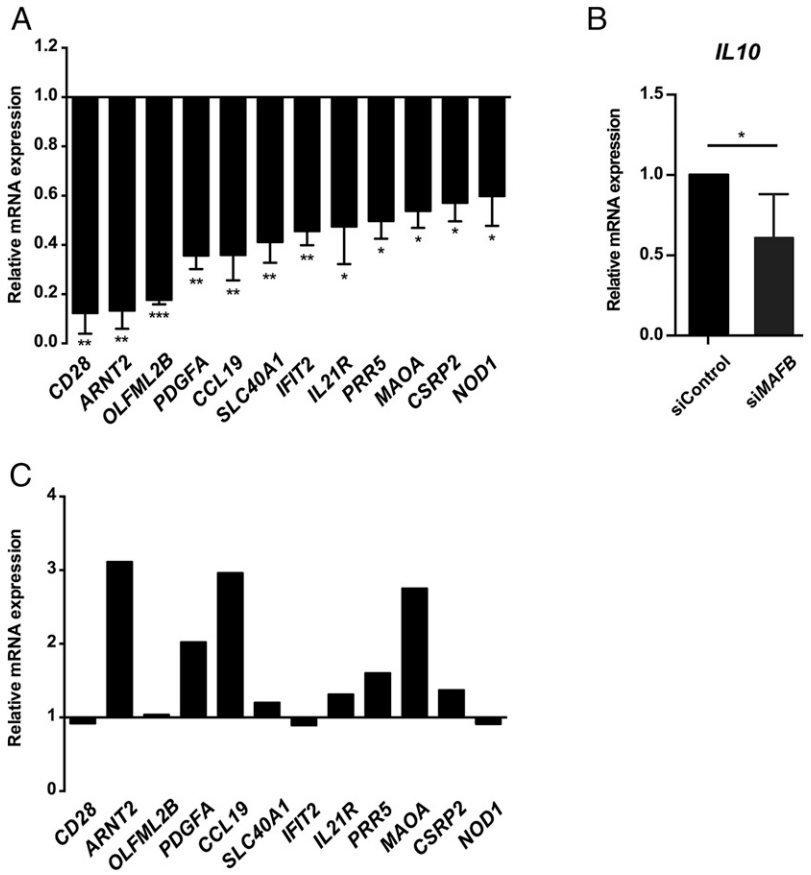

FIGURE 6. MAFB impacts the LPS response of M-MØ. (**A**) mRNA expression levels in LPS-treated (10 ng/ml, 4 h) siMAFB M-MØ, as determined by quantitative RT-PCR using custom-made microfluidic gene cards. Results are indicated as the mRNA levels of each gene in LPS-treated siMAFB M-MØ relative to LPS-treated siControl M-MØ ($n = 3$, $*p < 0.05$, $**p < 0.005$, $***p < 0.0005$). (**B**) *IL10* mRNA expression in LPS-treated siMAFB M-MØ as determined by quantitative RT-PCR. Results are shown relative to the *IL10* mRNA level detected in siControl-transfected LPS-treated M-MØ (arbitrarily set to 1) ($n = 5$, $*p < 0.05$). (**C**) mRNA expression levels in LPS-treated MCTO#1 M-MØ, as determined by quantitative RT-PCR. Results are indicated as the change in the expression of each gene in LPS-treated MCTO#1 M-MØ relative to the change of the same gene in LPS-treated control M-MØ.

gene) is required for the induction of T regulatory cells in peripheral tolerance (66) and whose expression depends on the Mafb-heterodimerizing factor c-Maf (27, 67). Conversely, MAFB negatively regulates genes associated with proinflammatory polarization like *CLEC5A*, which codes for a lectin preferentially expressed in TNF-α–producing macrophages in physiological and pathological settings (50). Gene ontology analysis further supports the link between MAFB expression and macrophage anti-inflammatory polarization, as MAFB knockdown leads to a global downregulation of genes preferentially expressed in anti-inflammatory macrophages (anti-inflammatory gene set) and to a significant upregulation of the proinflammatory gene set. Conversely, and in agreement with the higher $t_{1/2}$ of MCTO-causing MAFB mutants, the MCTO M-MØ gene signature revealed a global upregulation of the anti-inflammatory gene set. All of these findings indicate that MAFB is a critical determinant for the acquisition of the anti-inflammatory profile of human macrophages.

Our results on in vitro monocyte-derived macrophages clearly point to a link between M-CSF–driven differentiation and MAFB expression: M-CSF–driven macrophage differentiation results in high levels of MAFB, whereas the presence of GM-CSF lowers the basal levels of MAFB found in human monocytes. This result agrees with the ability of murine MafB to antagonize the phenotypic alteration of microglia induced by GM-CSF (68). Whether the MAFB/GM-CSF antagonism operates in all types of macrophages is still unknown. However, we have observed that MCTO mutations limit the acquisition of GM-CSF–inducible genes in GM-MØ, a finding that might be relevant in the case of macrophages whose development is critically dependent on GM-CSF (lung alveolar macrophages) (69). Although no lung-associated pathology has been to date reported in MCTO patients, it is worth noting that a significant number of genes aberrantly expressed in pulmonary diseases (pulmonary sarcoidosis, asthma, and tuberculosis) exhibit an altered expression in MCTO M-MØ, a finding that might be related to the fact that mature alveolar macrophages, identified as intermediate positive for the Emr1-encoded F4/80, are reduced in the bronchoalveolar lavage of mice expressing a dominant-negative MafB in macrophages (70). Given these antecedents, the analysis of further MCTO patients, it is certainly worthy as a means to get a deeper knowledge of the molecular mechanisms operating in this and other related osteolytic syndromes as well as to more clearly delineate the role of MAFB in the acquisition of the human macrophage anti-inflammatory profile.

Although we have used MCTO-derived macrophages as a tool to unravel the role of MAFB in human macrophage polarization, the

RT-PCR. Results from a single experiment are shown. (**G**) Schematic representation of the correlation between MAFB protein levels and the expression of GM-MØ– and M-MØ–specific genes in control and MCTO macrophages. (**H**) MCTO#1 and control osteoclasts, as determined by phase-contrast microscopy, on cells stained for TRAP. Two independent experiments were done on monocytes from the MCTO#1 patient, and one of them is shown. Original magnification ×40. (**I**) Relative mRNA expression of the indicated osteoclast-associated genes along the M-CSF + RANKL–induced osteoclast differentiation of monocytes from either two independent healthy controls (control) or the MCTO#1 patient. Shown are the mean (±SD) of the mRNA level of each gene at the indicated time points and relative to the mRNA level of the corresponding gene in M-CSF + RANKL–treated MCTO#1 monocytes at day 9. Results from a single experiment are shown. (**J**) Collagen-degradation activity of monocytes (from two healthy controls and the MCTO#1 patient) subjected to the M-CSF + RANKL–induced osteoclast differentiation procedure. Two experiments were performed with similar results, and one of them is shown. Empty and filled bars indicate monocytes differentiated in the presence of M-CSF alone or M-CSF + RANKL, respectively.

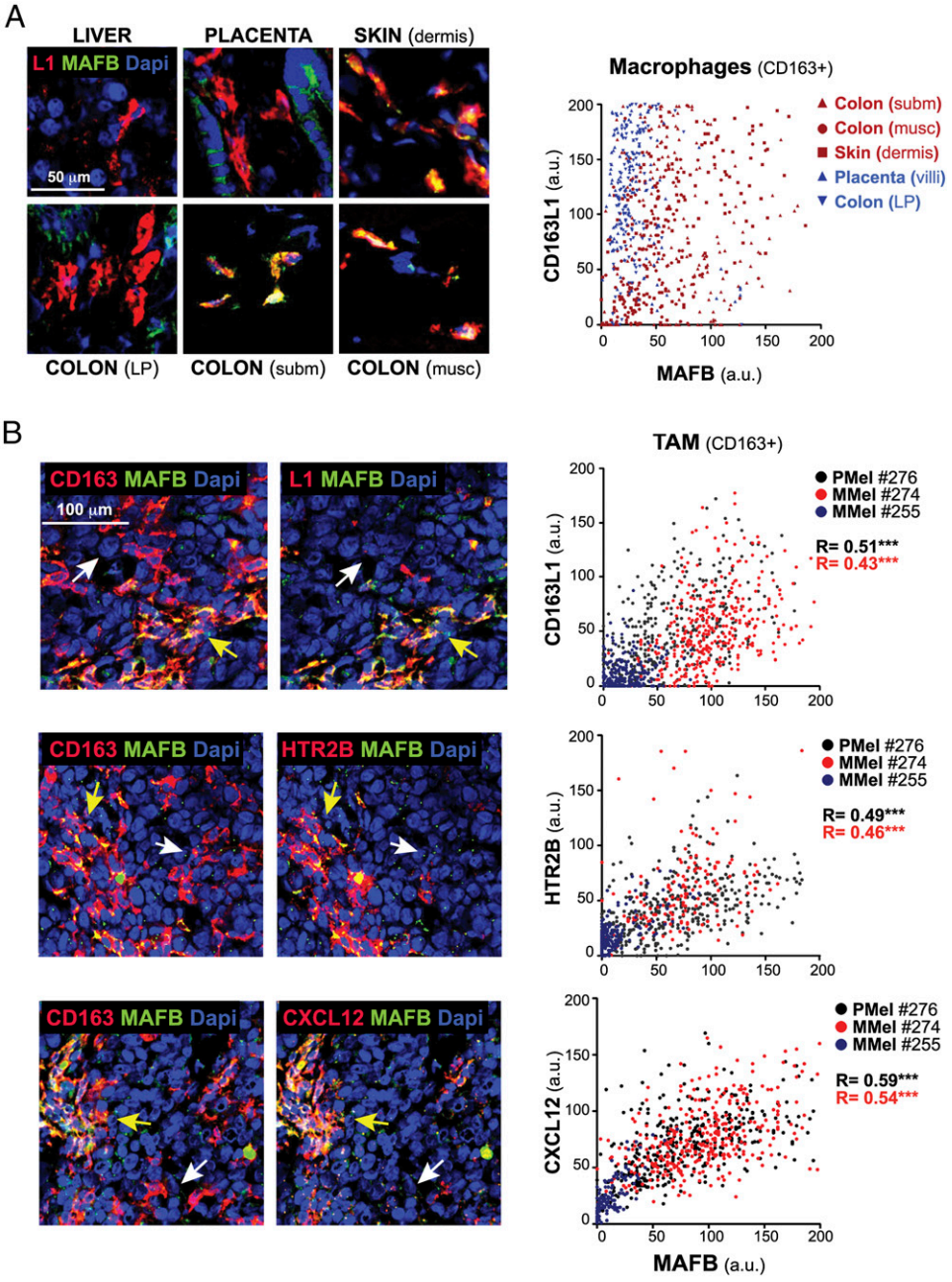

FIGURE 7. Human tissue-resident macrophages coexpress MAFB and MAFB-dependent genes. (**A**) Immunofluorescence of MAFB (green) and CD163L1 (L1, red) in tissues, as determined by confocal microscopy. Right panel: correlation between MAFB and CD163L1 expression in $CD163^+$ macrophages. Red and blue mark tissues with $CD163^+MAFB^+$ or $CD163^+MAFB^-$ macrophages, respectively. (**B**) Expression of the indicated proteins in samples of primary melanoma (PMel #276). Yellow arrows mark $CD163^+$ $MAFB^+$ $CD163L1^+$ $HTR2B^+$ $CXCL12^+$ macrophages, whereas white arrows mark $CD163^+$ $MAFB^-$ $CD163L1^-$ $HTR2B^-$ $CXCL12^-$ macrophages. Bottom panels show the positive correlation between MAFB expression and the expression of CD163L1, HTR2B, and CXCL12 in $CD163^+$ tumor-associated macrophages from primary melanoma (Pmel #276), lymph node metastatic melanoma (MMel #274), and skin metastatic melanoma (MMel #255) samples.

information we have gathered from MCTO monocytes/macrophages might shed light on the pathogenic mechanisms operating in MCTO and other diseases in which osteolysis is a defining pathological feature. In the case of MCTO, we have identified a number of genes whose expression is altered not only in MCTO-derived macrophages, but also in peripheral blood monocytes from the three analyzed MCTO patients (data not shown). Although analysis of additional patients is still required to propose their use as potential MCTO diagnostic markers, a disease commonly misdiagnosed (56), our results suggest that MCTO-causing mutations affect monocyte differentiation into tissue-resident macrophages, as exemplified by their inability to differentiate into functional osteoclasts in vitro. Whether the profound anti-inflammatory skewing of MCTO-derived M-MØ is responsible for their inability to generate osteoclasts in vitro is an issue that we are currently pursuing.

Acknowledgments

We gratefully acknowledge Dr. Lizbeth Estrada-Capetillo and Dr. Amaya Puig-Kröger for kindly providing useful reagents and samples.

Disclosures

The authors have no financial conflicts of interest.

References

1. Greter, M., I. Lelios, P. Pelczar, G. Hoeffel, J. Price, M. Leboeuf, T. M. Kündig, K. Frei, F. Ginhoux, M. Merad, and B. Becher. 2012. Stroma-derived interleukin-34 controls the development and maintenance of Langerhans cells and the maintenance of microglia. *Immunity* 37: 1050–1060.
2. Wang, Y., K. J. Szretter, W. Vermi, S. Gilfillan, C. Rossini, M. Cella, A. D. Barrow, M. S. Diamond, and M. Colonna. 2012. IL-34 is a tissue-restricted ligand of CSF1R required for the development of Langerhans cells and microglia. *Nat. Immunol.* 13: 753–760.
3. Hashimoto, D., A. Chow, C. Noizat, P. Teo, M. B. Beasley, M. Leboeuf, C. D. Becker, P. See, J. Price, D. Lucas, et al. 2013. Tissue-resident macrophages self-maintain locally throughout adult life with minimal contribution from circulating monocytes. *Immunity* 38: 792–804.
4. Epelman, S., K. J. Lavine, and G. J. Randolph. 2014. Origin and functions of tissue macrophages. *Immunity* 41: 21–35.
5. Mosser, D. M., and J. P. Edwards. 2008. Exploring the full spectrum of macrophage activation. *Nat. Rev. Immunol.* 8: 958–969.
6. Hamilton, J. A. 2008. Colony-stimulating factors in inflammation and autoimmunity. *Nat. Rev. Immunol.* 8: 533–544.

7. Verreck, F. A., T. de Boer, D. M. Langenberg, M. A. Hoeve, M. Kramer, E. Vaisberg, R. Kastelein, A. Kolk, R. de Waal-Malefyt, and T. H. Ottenhoff. 2004. Human IL-23-producing type 1 macrophages promote but IL-10-producing type 2 macrophages subvert immunity to (myco)bacteria. *Proc. Natl. Acad. Sci. USA* 101: 4560–4565.
8. Puig-Kröger, A., E. Sierra-Filardi, A. Domínguez-Soto, R. Samaniego, M. T. Corcuera, F. Gómez-Aguado, M. Ratnam, P. Sánchez-Mateos, and A. L. Corbí. 2009. Folate receptor beta is expressed by tumor-associated macrophages and constitutes a marker for M2 anti-inflammatory/regulatory macrophages. *Cancer Res.* 69: 9395–9403.
9. Sierra-Filardi, E., C. Nieto, A. Domínguez-Soto, R. Barroso, P. Sánchez-Mateos, A. Puig-Kroger, M. López-Bravo, J. Joven, C. Ardavín, J. L. Rodríguez-Fernández, et al. 2014. CCL2 shapes macrophage polarization by GM-CSF and M-CSF: identification of CCL2/CCR2-dependent gene expression profile. *J. Immunol.* 192: 3858–3867.
10. de las Casas-Engel, M., A. Domínguez-Soto, E. Sierra-Filardi, R. Bragado, C. Nieto, A. Puig-Kroger, R. Samaniego, M. Loza, M. T. Corcuera, F. Gómez-Aguado, et al. 2013. Serotonin skews human macrophage polarization through HTR2B and HTR7. *J. Immunol.* 190: 2301–2310.
11. Domínguez-Soto, A., E. Sierra-Filardi, A. Puig-Kröger, B. Pérez-Maceda, F. Gómez-Aguado, M. T. Corcuera, P. Sánchez-Mateos, and A. L. Corbí. 2011. Dendritic cell-specific ICAM-3-grabbing nonintegrin expression on M2-polarized and tumor-associated macrophages is macrophage-CSF dependent and enhanced by tumor-derived IL-6 and IL-10. *J. Immunol.* 186: 2192–2200.
12. Escribese, M. M., E. Sierra-Filardi, C. Nieto, R. Samaniego, C. Sánchez-Torres, T. Matsuyama, E. Calderon-Gómez, M. A. Vega, A. Salas, P. Sánchez-Mateos, and A. L. Corbí. 2012. The prolyl hydroxylase PHD3 identifies proinflammatory macrophages and its expression is regulated by activin A. *J. Immunol.* 189: 1946–1954.
13. Izquierdo, E., V. D. Cuevas, S. Fernández-Arroyo, M. Riera-Borrull, E. Orta-Zavalza, J. Joven, E. Rial, A. L. Corbi, and M. M. Escribese. 2015. Reshaping of human macrophage polarization through modulation of glucose catabolic pathways. *J. Immunol.* 195: 2442–2451.
14. Sierra-Filardi, E., A. Puig-Kröger, F. J. Blanco, C. Nieto, R. Bragado, M. I. Palomero, C. Bernabéu, M. A. Vega, and A. L. Corbí. 2011. Activin A skews macrophage polarization by promoting a proinflammatory phenotype and inhibiting the acquisition of anti-inflammatory macrophage markers. *Blood* 117: 5092–5101.
15. Lacey, D. C., A. Achuthan, A. J. Fleetwood, H. Dinh, J. Roiniotis, G. M. Scholz, M. W. Chang, S. K. Beckman, A. D. Cook, and J. A. Hamilton. 2012. Defining GM-CSF- and macrophage-CSF-dependent macrophage responses by in vitro models. *J. Immunol.* 188: 5752–5765.
16. Gordon, S., and F. O. Martinez. 2010. Alternative activation of macrophages: mechanism and functions. *Immunity* 32: 593–604.
17. Eychène, A., N. Rocques, and C. Pouponnot. 2008. A new MAFia in cancer. *Nat. Rev. Cancer* 8: 683–693.
18. Kataoka, K., K. T. Fujiwara, M. Noda, and M. Nishizawa. 1994. MafB, a new Maf family transcription activator that can associate with Maf and Fos but not with Jun. *Mol. Cell. Biol.* 14: 7581–7591.
19. Tillmanns, S., C. Otto, E. Jaffray, C. Du Roure, Y. Bakri, L. Vanhille, S. Sarrazin, R. T. Hay, and M. H. Sieweke. 2007. SUMO modification regulates MafB-driven macrophage differentiation by enabling Myb-dependent transcriptional repression. *Mol. Cell. Biol.* 27: 5554–5564.
20. Kim, K., J. H. Kim, J. Lee, H. M. Jin, H. Kook, K. K. Kim, S. Y. Lee, and N. Kim. 2007. MafB negatively regulates RANKL-mediated osteoclast differentiation. *Blood* 109: 3253–3259.
21. Reza, H. M., A. Urano, N. Shimada, and K. Yasuda. 2007. Sequential and combinatorial roles of maf family genes define proper lens development. *Mol. Vis.* 13: 18–30.
22. Dieterich, L. C., S. Klein, A. Mathelier, A. Sliwa-Primorac, Q. Ma, Y. K. Hong, J. W. Shin, M. Hamada, M. Lizio, M. Itoh, et al. 2015. DeepCAGE transcriptomics reveal an important role of the transcription factor MAFB in the lymphatic endothelium. *Cell Rep.* 13: 1493–1504.
23. Conrad, E., C. Dai, J. Spaeth, M. Guo, H. A. Cyphert, D. Scoville, J. Carroll, W. M. Yu, L. V. Goodrich, D. M. Harlan, et al. 2016. The MAFB transcription factor impacts islet α-cell function in rodents and represents a unique signature of primate islet β-cells. *Am. J. Physiol. Endocrinol. Metab.* 310: E91–E102.
24. Hang, Y., and R. Stein. 2011. MafA and MafB activity in pancreatic β cells. *Trends Endocrinol. Metab.* 22: 364–373.
25. Lopez-Pajares, V., K. Qu, J. Zhang, D. E. Webster, B. C. Barajas, Z. Siprashvili, B. J. Zarnegar, L. D. Boxer, E. J. Rios, S. Tao, et al. 2015. A LncRNA-MAF: MAFB transcription factor network regulates epidermal differentiation. *Dev. Cell* 32: 693–706.
26. Zhang, Y., and A. C. Ross. 2013. Retinoic acid and the transcription factor MafB act together and differentially to regulate aggrecan and matrix metalloproteinase gene expression in neonatal chondrocytes. *J. Cell. Biochem.* 114: 471–479.
27. Moriguchi, T., M. Hamada, N. Morito, T. Terunuma, K. Hasegawa, C. Zhang, T. Yokomizo, R. Esaki, E. Kuroda, K. Yoh, et al. 2006. MafB is essential for renal development and F4/80 expression in macrophages. *Mol. Cell. Biol.* 26: 5715–5727.
28. Morito, N., K. Yoh, M. Ojima, M. Okamura, M. Nakamura, M. Hamada, H. Shimohata, T. Moriguchi, K. Yamagata, and S. Takahashi. 2014. Overexpression of Mafb in podocytes protects against diabetic nephropathy. *J. Am. Soc. Nephrol.* 25: 2546–2557.
29. Kann, M., S. Ettou, Y. L. Jung, M. O. Lenz, M. E. Taglienti, P. J. Park, B. Schermer, T. Benzing, and J. A. Kreidberg. 2015. Genome-wide analysis of Wilms' tumor 1-controlled gene expression in podocytes reveals key regulatory mechanisms. *J. Am. Soc. Nephrol.* 26: 2097–2104.
30. Dong, L., S. Pietsch, Z. Tan, B. Perner, R. Sierig, D. Kruspe, M. Groth, R. Witzgall, H. J. Gröne, M. Platzer, and C. Englert. 2015. Integration of cistromic and transcriptomic analyses identifies Nphs2, Mafb, and Magi2 as Wilms' tumor 1 target genes in podocyte differentiation and maintenance. *J. Am. Soc. Nephrol.* 26: 2118–2128.
31. Kim, H., and B. Seed. 2010. The transcription factor MafB antagonizes antiviral responses by blocking recruitment of coactivators to the transcription factor IRF3. *Nat. Immunol.* 11: 743–750.
32. Lavin, Y., D. Winter, R. Blecher-Gonen, E. David, H. Keren-Shaul, M. Merad, S. Jung, and I. Amit. 2014. Tissue-resident macrophage enhancer landscapes are shaped by the local microenvironment. *Cell* 159: 1312–1326.
33. Sarrazin, S., N. Mossadegh-Keller, T. Fukao, A. Aziz, F. Mourcin, L. Vanhille, L. Kelly Modis, P. Kastner, S. Chan, E. Duprez, et al. 2009. MafB restricts M-CSF-dependent myeloid commitment divisions of hematopoietic stem cells. *Cell* 138: 300–313.
34. Soucie, E. L., Z. Weng, L. Geirsdottir, K. Molawi, J. Maurizio, R. Fenouil, N. Mossadegh-Keller, G. Gimenez, L. VanHille, M. Beniazza, et al. 2016. Lineage-specific enhancers activate self-renewal genes in macrophages and embryonic stem cells. *Science* 351: aad5510.
35. Dworschak, G. C., M. Draaken, A. Hilger, M. Born, H. Reutter, and M. Ludwig. 2013. An incompletely penetrant novel MAFB (p.Ser56Phe) variant in autosomal dominant multicentric carpotarsal osteolysis syndrome. *Int. J. Mol. Med.* 32: 174–178.
36. Mehawej, C., J. B. Courcet, G. Baujat, R. Mouy, M. Gérard, I. Landru, M. Gosselin, P. Koehrer, C. Mousson, S. Breton, et al. 2013. The identification of MAFB mutations in eight patients with multicentric carpo-tarsal osteolysis supports genetic homogeneity but clinical variability. *Am. J. Med. Genet. A* 161A: 3023–3029.
37. Mumm, S., M. Huskey, S. Duan, D. Wenkert, K. L. Madson, G. S. Gottesman, A. R. Nenninger, R. M. Laxer, W. H. McAlister, and M. P. Whyte. 2014. Multicentric carpotarsal osteolysis syndrome is caused by only a few domain-specific mutations in MAFB, a negative regulator of RANKL-induced osteoclastogenesis. *Am. J. Med. Genet. A* 164A: 2287–2293.
38. Zankl, A., E. L. Duncan, P. J. Leo, G. R. Clark, E. A. Glazov, M. C. Addor, T. Herlin, C. A. Kim, B. P. Leheup, J. McGill, et al. 2012. Multicentric carpotarsal osteolysis is caused by mutations clustering in the amino-terminal transcriptional activation domain of MAFB. [Published erratum appears in 2014 *Am. J. Hum. Genet.* 94: 643.] *Am. J. Hum. Genet.* 90: 494–501.
39. Stralen, E., R. J. Leguit, H. Begthel, L. Michaux, A. Buijs, H. Lemmens, J. M. Scheiff, C. Doyen, P. Pierre, F. Forget, et al. 2009. MafB oncoprotein detected by immunohistochemistry as a highly sensitive and specific marker for the prognostic unfavorable t(14;20) (q32;q12) in multiple myeloma patients. *Leukemia* 23: 801–803.
40. Lee, L. C., A. Y. Zhang, A. K. Chong, H. Pham, M. T. Longaker, and J. Chang. 2006. Expression of a novel gene, MafB, in Dupuytren's disease. *J. Hand Surg. Am.* 31: 211–218.
41. Park, J. G., M. A. Tischfield, A. A. Nugent, L. Cheng, S. A. Di Gioia, W. M. Chan, G. Maconachie, T. M. Bosley, C. G. Summers, D. G. Hunter, et al. 2016. Loss of MAFB function in humans and mice causes Duane syndrome, aberrant extraocular muscle innervation, and inner-ear defects. *Am. J. Hum. Genet.* 98: 1220–1227.
42. Hamada, M., M. Nakamura, M. T. Tran, T. Moriguchi, C. Hong, T. Ohsumi, T. T. Dinh, M. Kusakabe, M. Hattori, T. Katsumata, et al. 2014. MafB promotes atherosclerosis by inhibiting foam-cell apoptosis. *Nat. Commun.* 5: 3147.
43. Tran, M. T., M. Hamada, M. Nakamura, H. Jeon, R. Kamei, Y. Tsunakawa, K. Kulathunga, Y. Y. Lin, K. Fujisawa, T. Kudo, and S. Takahashi. 2016. MafB deficiency accelerates the development of obesity in mice. *FEBS Open Bio* 6: 540–547.
44. Sadl, V., F. Jin, J. Yu, S. Cui, D. Holmyard, S. Quaggin, G. Barsh, and S. Cordes. 2002. The mouse Kreisler (Krml1/MafB) segmentation gene is required for differentiation of glomerular visceral epithelial cells. *Dev. Biol.* 249: 16–29.
45. Hochberg, Y., and Y. Benjamini. 1990. More powerful procedures for multiple significance testing. *Stat. Med.* 9: 811–818.
46. Chen, E. Y., C. M. Tan, Y. Kou, Q. Duan, Z. Wang, G. V. Meirelles, N. R. Clark, and A. Ma'ayan. 2013. Enrichr: interactive and collaborative HTML5 gene list enrichment analysis tool. *BMC Bioinformatics* 14: 128.
47. Kuleshov, M. V., M. R. Jones, A. D. Rouillard, N. F. Fernandez, Q. Duan, Z. Wang, S. Koplev, S. L. Jenkins, K. M. Jagodnik, A. Lachmann, et al. 2016. Enrichr: a comprehensive gene set enrichment analysis web server 2016 update. *Nucleic Acids Res.* 44: W90–W97.
48. Subramanian, A., P. Tamayo, V. K. Mootha, S. Mukherjee, B. L. Ebert, M. A. Gillette, A. Paulovich, S. L. Pomeroy, T. R. Golub, E. S. Lander, and J. P. Mesirov. 2005. Gene set enrichment analysis: a knowledge-based approach for interpreting genome-wide expression profiles. *Proc. Natl. Acad. Sci. USA* 102: 15545–15550.
49. González-Domínguez, É., Á. Domínguez-Soto, C. Nieto, J. L. Flores-Sevilla, M. Pacheco-Blanco, V. Campos-Peña, M. A. Meraz-Ríos, M. A. Vega, A. L. Corbí, and C. Sánchez-Torres. 2016. Atypical activin A and IL-10 production impairs human CD16+ monocyte differentiation into anti-inflammatory macrophages. *J. Immunol.* 196: 1327–1337.
50. González-Domínguez, É., R. Samaniego, J. L. Flores-Sevilla, S. F. Campos-Campos, G. Gómez-Campos, A. Salas, V. Campos-Peña, A. L. Corbí, P. Sánchez-Mateos, and C. Sánchez-Torres. 2015. CD163L1 and CLEC5A discriminate subsets of human resident and inflammatory macrophages in vivo. *J. Leukoc. Biol.* 98: 453–466.
51. Kzhyshkowska, J., G. Workman, M. Cardó-Vila, W. Arap, R. Pasqualini, A. Gratchev, L. Krusell, S. Goerdt, and E. H. Sage. 2006. Novel function of

alternatively activated macrophages: stabilin-1-mediated clearance of SPARC. *J. Immunol.* 176: 5825–5832.
52. Henning, P., H. H. Conaway, and U. H. Lerner. 2015. Retinoid receptors in bone and their role in bone remodeling. *Front. Endocrinol. (Lausanne)* 6: 31.
53. Niceta, M., E. Stellacci, K. W. Gripp, G. Zampino, M. Kousi, M. Anselmi, A. Traversa, A. Ciolfi, D. Stabley, A. Bruselles, et al. 2015. Mutations impairing GSK3-mediated MAF phosphorylation cause cataract, deafness, intellectual disability, seizures, and a down syndrome-like facies. *Am. J. Hum. Genet.* 96: 816–825.
54. Rocques, N., N. Abou Zeid, K. Sii-Felice, L. Lecoin, M. P. Felder-Schmittbuhl, A. Eychène, and C. Pouponnot. 2007. GSK-3-mediated phosphorylation enhances Maf-transforming activity. *Mol. Cell* 28: 584–597.
55. Anta Martínez, L., A. Vieitez Rey, S. Pombo Expósito, and F. Sines Castro. 2011. Osteolisis Carpo-Tarsal Multicéntrica. In *XX Congreso Hispano Luso de Cirugía de la mano*. GEYSECO Ed., Valencia, Spain, p. 152.
56. Faber, M. R., R. Verlaak, T. J. Fiselier, B. C. Hamel, M. J. Franssen, and G. P. Gerrits. 2004. Inherited multicentric osteolysis with carpal-tarsal localisation mimicking juvenile idiopathic arthritis. *Eur. J. Pediatr.* 163: 612–618.
57. Ruffell, B., and L. M. Coussens. 2015. Macrophages and therapeutic resistance in cancer. *Cancer Cell* 27: 462–472.
58. Rivollier, A., J. He, A. Kole, V. Valatas, and B. L. Kelsall. 2012. Inflammation switches the differentiation program of Ly6Chi monocytes from antiinflammatory macrophages to inflammatory dendritic cells in the colon. *J. Exp. Med.* 209: 139–155.
59. Okabe, Y., and R. Medzhitov. 2016. Tissue biology perspective on macrophages. *Nat. Immunol.* 17: 9–17.
60. Gosselin, D., V. M. Link, C. E. Romanoski, G. J. Fonseca, D. Z. Eichenfield, N. J. Spann, J. D. Stender, H. B. Chun, H. Garner, F. Geissmann, and C. K. Glass. 2014. Environment drives selection and function of enhancers controlling tissue-specific macrophage identities. [Published erratum appears in 2015 *Cell* 160: 351.] *Cell* 159: 1327–1340.
61. Schultze, J. L. 2016. Reprogramming of macrophages: new opportunities for therapeutic targeting. *Curr. Opin. Pharmacol.* 26: 10–15.
62. Gabryšová, L., A. Howes, M. Saraiva, and A. O'Garra. 2014. The regulation of IL-10 expression. *Curr. Top. Microbiol. Immunol.* 380: 157–190.
63. Suzuki, H. I., M. Arase, H. Matsuyama, Y. L. Choi, T. Ueno, H. Mano, K. Sugimoto, and K. Miyazono. 2011. MCPIP1 ribonuclease antagonizes dicer and terminates microRNA biogenesis through precursor microRNA degradation. *Mol. Cell* 44: 424–436.
64. Matsushita, K., O. Takeuchi, D. M. Standley, Y. Kumagai, T. Kawagoe, T. Miyake, T. Satoh, H. Kato, T. Tsujimura, H. Nakamura, and S. Akira. 2009. Zc3h12a is an RNase essential for controlling immune responses by regulating mRNA decay. *Nature* 458: 1185–1190.
65. Zhang, Y., Q. Chen, and A. C. Ross. 2012. Retinoic acid and tumor necrosis factor-α induced monocytic cell gene expression is regulated in part by induction of transcription factor MafB. *Exp. Cell Res.* 318: 2407–2416.
66. Lin, H. H., D. E. Faunce, M. Stacey, A. Terajewicz, T. Nakamura, J. Zhang-Hoover, M. Kerley, M. L. Mucenski, S. Gordon, and J. Stein-Streilein. 2005. The macrophage F4/80 receptor is required for the induction of antigen-specific efferent regulatory T cells in peripheral tolerance. *J. Exp. Med.* 201: 1615–1625.
67. Nakamura, M., M. Hamada, K. Hasegawa, M. Kusakabe, H. Suzuki, D. R. Greaves, T. Moriguchi, T. Kudo, and S. Takahashi. 2009. c-Maf is essential for the F4/80 expression in macrophages in vivo. *Gene* 445: 66–72.
68. Koshida, R., H. Oishi, M. Hamada, and S. Takahashi. 2015. MafB antagonizes phenotypic alteration induced by GM-CSF in microglia. *Biochem. Biophys. Res. Commun.* 463: 109–115.
69. Shibata, Y., P. Y. Berclaz, Z. C. Chroneos, M. Yoshida, J. A. Whitsett, and B. C. Trapnell. 2001. GM-CSF regulates alveolar macrophage differentiation and innate immunity in the lung through PU.1. *Immunity* 15: 557–567.
70. Aida, Y., Y. Shibata, S. Abe, S. Inoue, T. Kimura, A. Igarashi, K. Yamauchi, K. Nunomiya, H. Kishi, T. Nemoto, et al. 2014. Inhibition of elastase-pulmonary emphysema in dominant-negative MafB transgenic mice. *Int. J. Biol. Sci.* 10: 882–894.